Published in final edited form as:
Colloids Surf B Biointerfaces. 2014 July 1; 119: 106–114. doi:10.1016/j.colsurfb.2014.04.027.

Effect of PEG Molecular Weight on Stability, T_2 contrast, Cytotoxicity, and Cellular Uptake of Superparamagnetic Iron Oxide Nanoparticles (SPIONs)

Yoonjee C. Park[§,1], **Jared B. Smith**[§,1,$], **Tuan Pham**[1], **Ragnhild D. Whitaker**[1,#], **Christopher A. Sucato**[1,€], **James A. Hamilton**[2], **Elizabeth Bartolak-Suki**[1], and **Joyce Y. Wong**[1]

[1]Department of Biomedical Engineering, Boston University, 44 Cummington Mall, Boston, MA 02215, USA

[2]Department of Physiology and Biophysics, Boston University School of Medicine, 700 Albany Street, Boston, MA 02118

Abstract

Superparamagnetic iron oxide nanoparticles (SPIONs) are currently unavailable as MRI contrast agents for detecting atherosclerosis in the clinical setting because of either low signal enhancement or safety concerns. Therefore, a new generation of SPIONs with increased circulation time, enhanced image contrast, and less cytotoxicity is essential. In this study, monodisperse SPIONs were synthesized and coated with polyethylene glycol (PEG) of varying molecular weights. The resulting PEGylated SPIONs were characterized, and their interactions with vascular smooth muscle cells (VSMCs) were examined. SPIONs were tested at different concentrations (100 and 500 ppm Fe) for stability, T_2 contrast, cytotoxicity, and cellular uptake to determine an optimal formulation for *in vivo* use. We found that at 100 ppm Fe, the PEG 2K SPIONs showed adequate stability and magnetic contrast, and exhibited the least cytotoxicity and nonspecific cellular uptake. An increase in cell viability was observed when the SPION-treated cells were washed with PBS after one hour incubation compared to 5 and 24 hour incubation without washing. Our investigation provides insight into the potential safe application of SPIONs in the clinic.

Keywords

superparamagnetic iron oxide nanoparticles; coating; stability; T_2 relaxation; toxicity; particle internalization

Correspondence to: Joyce Y. Wong.
[§]Co-first authors
[$]Present Addresses: College of Medicine, University of Florida, 1600 Southwest Archer Road, Gainesville, FL 32603
[#]ScandiDerma AS, Sykehusveien 23, Tromsoe, Norway
[€]Blue Stream Laboratories, 763 Concord Ave, Bldg E, Cambridge, MA 02138

Conflict of Interest

1. Introduction

Cardiovascular disease (CVD) remains the leading cause of death in the United States, claiming over half a million lives annually.[1] One of the most common precursors to CVD is atherosclerosis,[2–4] thus there is a great need for diagnostic tools that detect atherosclerosis. Magnetic resonance angiography (MRA) is often used for diagnosing CVD, both with or without contrast agents. A major contrast agent for magnetic resonance imaging (MRI) is superparamagnetic iron oxide nanoparticles (SPIONs), which are currently used clinically for perfusion, but not yet for atherosclerosis imaging. SPIONs shorten T_2 relaxation times because of their very large magnetic moment, which leads to local magnetic field inhomogeneity[5] that causes its dark appearance on MR images.[6] Unfortunately, SPIONs for MRA are currently unavailable commercially because of either low signal enhancement or safety concerns.[7] Therefore, a new generation of SPIONs for MRA with increased circulation time, enhanced image contrast, and less cytotoxicity is essential.

Successful application of a SPION-based contrast agent is dependent on multiple properties, including its size, size distribution, shape, magnetic susceptibility, and surface modification,[6, 8–10] because the nuclear magnetic resonance (NMR) T_2 signal is very sensitive to these parameters. The interaction between the particle and biomacromolecule or cell *in vivo* is also affected by these parameters, especially size and surface modification. For example, adsorption of serum on a particle could strongly inhibit cellular uptake.[11]

The polyethylene glycol (PEG) coating of SPIONs provides stability between the particles via steric repulsion,[12] and reduces undesired interactions with plasma proteins and their subsequent opsonization.[13] PEG also allows targeting ligands to be conjugated onto the SPIONs.[9] Clariscan™ (NC100150), a preclinical MRA agent, consists of superparamagnetic iron oxide crystals of a magnetite/maghemite with low-molecular-weight (MW) polyethylene glycol (PEG) coating on a carbohydrate residue. However, the development was discontinued because of safety issues. In this study, we examined the effect of the PEG MW on the nanoparticle interactions with cells by synthesizing SPIONs with various MWs of PEG chains on the nanoparticle surface.

Additionally, to use PEG-coated SPIONs as MRI contrast agents, we must study the effect of the PEG coating on magnetic properties of SPIONs. Several studies have demonstrated effects of various PEG coatings on T_2 relaxivity; however, the reported effects are inconsistent and state maximum T_2 relaxivities at contradicting PEG MW values.[9, 10] Furthermore, the study of the effect of SPION concentration on relaxivity for clinical purposes has not yet been reported, although the concentration is known to significantly affect T_2 relaxivity. In this study, we investigate nanoparticle concentrations with various PEG MW coatings that can provide sufficient contrast.

Lastly, cytotoxicity and cellular uptake of various PEG-coated SPIONs at different concentrations has yet to be reported.[14] Here, we report an optimal combination of PEG MW and concentration for diagnosing atherosclerosis, with a focus on interactions with vascular smooth muscle cells (VSMCs). As atherosclerosis progresses, VSMCs proliferate

and migrate from the tunica media into the intima in response to cytokines secreted by damaged endothelial cells. Therefore, imaging with MR (magnetic resonance) using SPIONs targeted to VMSCs would be a powerful way to diagnose disease progression. As a prerequisite to a targeting study, we first examine SPION cytotoxicity to VSMCs by monitoring its nonspecific binding or cellular uptake.

A major goal of this study is to characterize the size, composition, and magnetic properties of the SPIONs with various molecular weights of PEG chains on the particle surface. Additionally, we analyze particle stability as a function of PEG MWs at different conditions of pH, ionic strength, and presence of biomacromolecules, and evaluate their cytotoxic and morphological effects on VSMCs with and without washing SPIONs to mimic clearance due to arterial blood flow. Finally, we determine the optimal nanoparticle design by considering all of these effects.

2. Materials and Methods

2.1. Materials

Iron tri(acetylacetonate) (2 mmol), 1,2-tetradecanediol (10 mmol), oleic acid (6 mmol), oleylamine (6 mmol), dibenzyl ether, citric acid, diethyl ether, 2-methoxyethylamine, N-(3-Dimethylaminopropyl)-N′-ethylcarbodiimide hydrochloride (EDC), N-Hydroxysuccinimide (NHS), thioglycolic acid, hydroxylamine, and phenanthroline were all purchased from Sigma-Aldrich (St. Louis, Missouri). 1,2-dichlorobenzene and N,N'-dimethylformamide were from Acros Organics (Morris Plains, New Jersey). NH_2-PEG (550 Da, 2000 Da, 5000 Da, and 10000 Da) were all obtained from Laysan Bio, Inc. (Arab, Alabama). Slide-A-Lyzer G2 dialysis cassettes, chambered slides, bovine calf serum (BCS) were acquired from Thermo Scientific (Rockford, Illinois). Dulbecco's Modified Eagle's Medium (DMEM), Dulbecco's Phosphate Buffer Saline (DPBS), penicillin, and streptomycin were purchased from Gibco Life Technologies, Inc. (NY, USA).

2.2. Superparamagnetic Iron Oxide (Fe_3O_4) Nanoparticle (SPION) Synthesis

SPIONs were synthesized by a method presented by Sun et al. and further modified following a method described by Lattuada et al. [15] The detailed procedure is described in our previous study.[12] Briefly, iron(III) tri(acetylacetonate) [$Fe(acac)_3$] (2 mmol), benzyl ether (40 mL), 1,2-tetradecanediol (10 mmol), oleic acid (6 mmol), and oleylamine (6 mmol) were mixed and stirred magnetically under a flow of nitrogen. The mixture was heated at 2 degrees per min to 100 °C and kept for 45 min, followed by heating to 200 °C at 2 degrees per min and kept for 2 h. Subsequently the reaction mixture was heated to reflux (∼ 300 °C) and held for another 30 min to 1 h. The oleic acid – coated SPIONs were stored after washing steps with an excess of ethanol and after a drying step in a vacuum oven. For hydrophilic water-soluble SPIONs, oleic acid – coated nanoparticles were dissolved in a dichlorobenzene and dimethylformamide mixture (1:1 v/v) with citric acid and heated to 100 °C for 24 h. Finally, the citric acid-coated SPIONs were further functionalized with amine-terminated polyethylene glycol (PEG) of varying chain lengths (550, 2000, 5000, and 10000 Da) or 2-methoxyethylamine (2-MEA) using N-hydroxysuccinimide (NHS) ester and 1-ethyl-3-(3-dimethylaminopropyl) carbodiimide (EDC) in pH 9 for 24 h on an agitator at

room temperature. The PEG Fe NPs were obtained after they were dialyzed for 48 h against deionized water at pH 9.

2.3. Size Measurements – TEM and DLS

The shape and size of the SPIONs were examined on a JEOL 2100 (200 kV) transmission electron microscope (Tokyo, Japan). The samples were prepared by placing a few drops of nanoparticle suspension onto a standard carbon-coated copper grid and then dried at ambient conditions. The TEM images were processed in ImageJ (NIH) to determine particle size and size distribution. Dynamic light scattering (DLS) measurements were performed at a wavelength λ of 659 nm at 25 °C with Brookhaven 90Plus (Brookhaven Instrument, Holtsville, NY). Three 2 min measurements were taken for each sample. The average size and size distribution obtained from both methods were compared.

2.4. Carbon, Nitrogen, and Hydrogen Elemental Analysis

The SPION samples were evaluated by Intertek QTI Laboratory (Whitehouse, New Jersey) for carbon, nitrogen, and hydrogen combustion elemental analysis. We quantitatively analyzed the nanoparticle surface chemistry for different PEG molecular weights based on the percentage of carbon loss (% carbon).

2.5. Thermogravimetric Analysis (TGA)

TGA was performed using a TA Instruments Q500 thermogravimetric analyzer (New Castle, Delaware). Approximately 2 mg of each nanoparticle sample was dried using a vacuum oven and analyzed from 25°C − 500°C under nitrogen. The surface chemistry of SPIONs was calculated based on total weight loss of the surface coating. Particles stored for 7 days in pH 9 buffer solution (I=0.029), DMEM-serum or DMEM alone were evaluated for percent weight loss. The surface chemistry calculations based on TGA results were compared to those obtained via elemental analysis.

2.6. T_2 Relaxation Measurements

Spin-spin relaxation times (T_2) were measured at Fe concentration of 10 ppm, 50 ppm, 100 ppm, and 500 ppm in deionized water. These samples were placed in glass capillary sample tubes, and T_2 values were determined by using a Bruker nuclear magnetic resonance (NMR) spectrometer (Billerica, Massachusetts). NMR images and T_2 values were obtained at a magnetic field of 11.7 T, and a proton frequency of 500 mHz.

2.7. Stability Measurements

Stability of SPIONs in pH 9 buffer solution was analyzed by measuring size with DLS over a 12 h period immediately after particle synthesis was complete. The pH 9 buffer solution was chosen because SPIONs show best stability against aggregation at pH 9 in the range of pH 3 to 11. This experiment was repeated for 2-methoxyethylamine-coated SPIONs (2-MEA SPIONs) and PEGylated (MW 2000 and 10,000) SPIONs (PEG 2K SPIONs and PEG 10K SPIONs, respectively) kept in DMEM with and without 10% BCS, in order to evaluate the effect of serum similar to what is found in blood. SPIONs dispersed in pH 9 buffer solution were isolated using an Amicon Ultra Centrifugal Filter (Millipore, Billerica,

Massachusetts) and transferred to either a DMEM or a DMEM + BCS solution of equal volume.

2.8. Zeta(ζ)-potential Measurements

SPION dispersions were measured at 25 °C with a Brookhaven 90Plus, using the software PALS Zeta Potential Analyzer. Each measurement consisted of 20 cycles, and five measurements were made for each sample.

2.9. SPION Dispersion Concentration Determination

A colorimetric assay was carried out to determine Fe concentration in SPIONs. 1 μl of thioglycolic acid was added to 1 mL of a pH 9 SPION solution, reducing Fe^{3+} to Fe^{2+}. After overnight incubation, 100 μL of reduced Fe^{2+} solution was transferred to a microcentrifuge tube with 5 μl of 2.5% sodium citrate, 100 μl of 10% hydroxylamine, and 150 μl 0.25% phenanthroline. Absorbance was measured at 510 nm using a Molecular Devices SpectraMax M5 (Sunnyvale, California). The final Fe concentration was calculated using a calibration curve.

2.10. Cell Viability Assay

Bovine vascular smooth muscle cells (VSMCs) seeded at 8000 cells/cm^2 were used for cell viability tests of SPIONs. Cells were cultured in high glucose DMEM supplemented with 10% BCS, 1% L-glutamine, and 1% penicillin-streptomycin at 37 °C, 5% carbon dioxide. All experiments were done at cell passages 12–16. Cell viability after exposure to SPIONs was determined by using the LIVE/DEAD Viability/Cytotoxicity Kit for mammalian cells (Gibco Life Technologies, Inc., NY, USA). Particle toxicity was evaluated at three distinct time points (5, 10, and 24 h) and at three different concentrations (100, 500, and 1000 ppm Fe) for 2-methoxyethylamine (2-MEA), PEG 2K, and PEG 10K in DMEM in triplicate. In order to mimic nanoparticle clearance due to circulation, VSMCs were incubated with SPIONs (2-MEA, PEG 2K, and PEG 10K) at 100 ppm and 500 ppm of Fe in DMEM plus 10% BCS (DMEM + BCS) for 1h and then washed with DPBS. The DMEM + BCS solution was then placed on cells, and the LIVE/DEAD Viability/Cytotoxicity Kit was used to evaluate cell viability 23h later.

2.11. Evaluation of SPION Uptake

Prussian blue staining kit (Electron Microscopy Sciences, Hartfield, PA) was performed to evaluate uptake and cellular distribution of SPIONs in VSMCs. Cells were seeded at 8000 cells/cm^2 on chambered slides (Thermo Scientific) and incubated with SPIONs for 1 hr and 5 hr at 100 and 500 ppm Fe. Cellular uptake kinetic studies have shown that the uptake rate gradually slows down and reaches a plateau around 5 h.[16, 17] After SPION incubation at 37 °C, slides were washed with DPBS and deionized water. The Prussian blue solution consisting of equal parts of 20% hydrochloric acid and 10% potassium ferrocyanide solution was added for 20 min, and then slides were washed three times with deionized water. The slides were then counter-stained with Nuclear fast red (Vector Laboratories, Peterborough, UK) for 5 min and washed again with deionized water (two times). The cells were dehydrated with 95% and 100% ethanol (two changes), and two 3 min washes with xylene.

Finally, slides were mounted and imaged with bright field microscopy (Nikon Eclipse 50i, Nikon Instruments Inc., Melville, N.Y.).

3. Results

3.1. SPION Characterization - Size, Surface Chemistry and Magnetic Properties

3.1.1. TEM and DLS results—Citric acid-coated SPIONs (CA SPIONs), 2-methoxyethyleneamine-coated SPIONs (2-MEA SPIONs), and PEGylated SPIONs (PEG SPIONs) were characterized with several different methods to determine individual particle size, surface chemistry, and magnetic properties. TEM images of SPIONs produced in our previous studies with the same method showed that CA SPIONs and PEG 2K SPIONs consisted of iron oxide cores of 6–11 nm and 5– 11 nm in diameter, respectively, and average diameter from TEM images were both 8 nm (Figure 1 in Ref.12). Polydispersity of CA SPIONs and PEG 2K SPIONs was 14% and 27%, respectively, indicating that size distribution of the CA SPIONs is narrow. Average hydrodynamic effective diameters of CA SPIONs and PEG 2K SPIONs, measured by dynamic light scattering (DLS) at a particle concentration of 100 ppm Fe, were 120 nm and 145 nm, respectively. Size range between 10% and 90% of the total distribution calculated based on Gaussian distribution was 108–132 nm and 132–158 nm, respectively. Compared to TEM results, the average diameters measured by DLS were larger. This may be due in part to flocculation of the particles. In Ref. 12, the average diameters of the same kind of particles measured by DLS after a short bath sonication (~ 30 s) were 46 nm and 64 nm for CA SPIONs and PEG 2K SPIONs, respectively. Thus it is likely that the average diameters of flocculates of two to three particles were measured by DLS. The other reason why the average size measured by DLS is larger than the one observed by TEM is because DLS measures hydrodynamic diameters which is a hypothetical hydrated sphere that diffuses with the same speed as the particle under examination.[18] Other SPIONs (2-MEA, PEG 550, PEG 5K, and PEG 10K SPIONs) all showed similar hydrodynamic diameters from 100–150 nm (See data for 0 h in Table 3).

3.1.2. Elemental Analysis and Thermogravimetric Analysis (TGA) results—Surface chemistry of SPIONs was characterized and confirmed by elemental analysis and thermogravimetric analysis (TGA) (Table 1 and Table 2, respectively). For elemental analysis, the number of molecules grafted to the surface via carboxylate groups of citric acid per nanoparticle was calculated based on the percentage of carbon (% carbon) burned. It was determined that the number of molecules and surface density of these molecules on SPIONs with average size of 8 nm in diameter decreased as the coating molecular weight increased. The distance between grafting sites calculated from the surface density clearly supports this trend.

Comparable results for the surface chemistry of various SPIONs were also obtained from TGA, which showed that the surface density decreases as PEG MW increases. TGA was used to study surface chemistry of SPIONs in physiologically relevant conditions to investigate the effect of adsorption of ions or molecules, such as glucose or serum proteins, on the particle surface. The pH 9 buffer solution was used as a comparison to other physiologically relevant buffers because the final product of PEGylated SPIONs was

obtained at pH 9, and SPIONs are stable at pH 9 for years (data no shown). The 2-MEA and PEG 2K SPIONs stored in DMEM solution showed approximately 10% more weight loss than ones stored in pH 9 buffer solution, indicating adsorption of ions or molecules onto the surface. As SPION stability results (Table 3) show, all three types of SPIONs aggressively aggregate in DMEM with time (~1000 nm after 12 h). The aggregation may have caused confinement of the PEG coating and a lower percentage of weight loss, especially for PEG 10K SPIONs. SPIONs stored in DMEM with BCS (DMEM + BCS) show much higher percentage of weight loss for 2-MEA and PEG 2K SPIONs, implying adsorption of serum proteins.

3.1.3. T_2 relaxation results—The spin-spin relaxations (T_2) of the SPIONs with various MWs of PEG coating were measured at different concentrations. In Figure 1 (A), 500 ppm Fe show no difference in T_2 MR images brightness among the samples, even at an earlier echo time than 100 ppm Fe (6.4 ms vs. 19.1 ms at 100 ppm Fe), indicating the SPIONs signals are saturated at this higher concentration. Figure 1 (B) shows that the T_2 relaxation rate ($1/T_2$) increases linearly with iron concentration up to 100 ppm Fe, and the slope decreases above 100 ppm Fe, which may be due to saturation, as shown in Figure 1 (A).

The relaxivity (R_2), which is the slope of $1/T_2$ to iron concentration, decreases with PEG MW (Figure 1 (C)). The values for 2-MEA, PEG 550, 2K, 5K, and 10K were 1.049, 0.8379, 0.7021, 0.8176, and 0.6456 $s^{-1}ppm^{-1}$, respectively. The values were obtained by fitting slopes from 10 to 100 ppm Fe with an intercept at 0.48 which is $1/T_2$ value of water. Except for PEG 5K, relaxivity decreases as PEG MW increases, indicating that the thickness of PEG coating at the particle surface affects T_2 relaxivity.

3.2. SPION Stability

Stability of SPIONs functionalized with 2-MEA, PEG 2K and PEG 10K in pH 9 buffer solution, DMEM, and DMEM+BCS (pH 7.4) at concentrations of 100ppm Fe and 500ppm Fe was studied using dynamic light scattering (DLS). The three kinds of SPIONs were stable in pH 9 buffer solution, where they maintain a consistent hydrodynamic diameter (D_H) over 12 h analysis. We found that concentration does not have an effect on the measured hydrodynamic diameter in pH 9 buffer solution. In contrast, SPIONs in DMEM for all three different coatings appeared to be less stable than those stored in pH 9 buffer solution. D_H values instantly increased four to six times larger (at 0 h) compared to samples in pH 9 solution, and grew by approximately 300 nm over 12 h. Interestingly, D_H increased rapidly between 0 and 2 h and plateaued from 2 to 12 h. Also, the effect of SPION concentration was observed in DMEM. When 500 ppm Fe was tested, D_H values were 800–900 nm for all three types of PEG-coated SPIONs at 0 h, which were larger than at 100 ppm Fe by 200–400 nm. The rate of D_H increase after 0 h at 500 ppm Fe was, however, slower than at 100 ppm Fe, especially for PEG 10K. When SPIONs were dispersed in DMEM with 10% serum, D_H values were around 200 nm over the 12 h period, regardless of PEG MW or concentration of nanoparticles, indicating the serum has a stabilizing effect.

3.3. Cytotoxicity of SPIONs

The effect of SPIONs functionalized with different PEG MWs, and with two different concentrations on VSMCs was tested with a cytotoxicity assay and time-lapse study over 24 h. We extended these studies by adding a washing step to simulate clearance of nanoparticles due to blood flow in the arteries. Cells were exposed for 1 h and then washed and replaced with fresh media for the next 23 h. The cell cytotoxicity (Live/Dead) assay results showed that the fraction of live cells with 100 ppm Fe of SPIONs in general was approximately 20% greater than those exposed to 500 ppm Fe, especially for PEG 2K SPIONs ($p = 0.071$ for PEG 2K) (Figure 2). For example, after 24 h, the fraction of live cells with PEG 2K SPION at 100 ppm Fe was about 0.2 greater than at 500 ppm Fe. In terms of the effect of PEG MW, PEG 2K also showed substantially higher cell viability compared to 2-MEA or PEG 10K especially at 100 ppm Fe ($p=0.017$ for 2-MEA vs PEG 2K; $p=0.011$ for PEG 2K vs. PEG 10K). When nanoparticle clearance is simulated by washing, the fraction of viable cells significantly improved by approximately 0.2 for all kinds of particles tested after 24 h especially at 500 ppm Fe ($p=0.011$). PEG 2K SPIONs at 100 ppm Fe showed minimal cell loss (1–2%) with this condition.

The time-lapse study showed that when cells were exposed to 100 ppm Fe of SPIONs for 24 h, all three types of SPIONs had no substantial effect on cell morphology or proliferation (Figure 3). However, at 500 ppm Fe, inhibition of cell proliferation was observed over 24 h for all three SPIONs. In time-lapse movies, cells were unable to attach to the culture dish surface (data not shown), resulting in cell death at 500 ppm Fe. When SPION clearance was simulated (washed), cell motility significantly improved, especially for 500 ppm Fe. Cell dimensional characteristics from time-lapse images have been analyzed quantitatively to support cell viability results from the live/dead assay (Figure 4). Although the method used is inaccurate for determining cell viability, others have attempted to explain cell proliferation or viability by analyzing dimensional parameters, such as cell area or cell perimeter.[19, 20] The images at 24 h (T_{24h}) from Figure 3 were captured, and the whole cell area and perimeter in each image were processed to compare the effect of SPION concentration and washing on cells.

The whole cell areas of VSMCs when exposed to 500 ppm Fe of SPIONs were approximately seven times less than when they were exposed to 100 ppm Fe of SPIONs, which indicates either that cells do not spread out or that they do not survive in the presence of particles. On the other hand, when cells were washed after 1 h exposure, cell areas for 500 ppm Fe were comparable to areas found for 100 ppm Fe. Notably, the effect of washing was much more remarkable for 500 ppm Fe than 100 ppm Fe. Similarly, although whole cell perimeters when exposed to 500 ppm Fe were about half of the value for 100 ppm Fe exposure, washing led to comparable cell perimeter values for 500 and 100 ppm Fe.

3.4 Cellular uptake of SPIONs

Cellular uptake of SPIONs in VSMCs was measured using a Prussian blue assay (Figure 5). Visually, incubation at 5 h showed a significant amount of SPIONs internalized compared to 1 h incubation for both concentrations of SPIONs. For 1 h incubation time at 100 ppm Fe of SPIONs, cell uptake was minimal. On the other hand, some nanoparticles inside cells were

observed at 500 ppm Fe for all three types of SPIONs. After 5 h, SPIONs covered the perinuclear region of VSMCs for 100 ppm Fe, which was even more apparent at 500 ppm Fe.

4. Discussion

Various SPIONs were examined at two different concentrations to determine an optimal combination of PEG MW coating and SPION concentration for use as an MRI contrast agent in atherosclerosis. Based on their stability, magnetic properties, cytotoxicity, and cellular uptake behaviors, PEG 2K SPIONs at a concentration of 100 ppm Fe was the best among the cases tested.

Characterizing SPIONs is important because the size or surface composition influences nanoparticle efficacy for clinical application of interest, i.e. cellular uptake. SPIONs measured by DLS were approximately 120–140 nm in diameter, which is comparable to Feridex, the most commonly used MRI contrast agent for liver or spleen imaging. The individual particle size, 8 nm in diameter, determined by TEM images, is still small enough to have superparamagnetism and to penetrate cell membranes, making it favorable for targeted molecular imaging or for use as drug delivery vehicles.[21]

In the context of maintaining individual dispersed particles for these applications, colloidal stability of SPIONs against aggregation in physiological conditions is important. Moreover, stability affects magnetic properties and toxicity *in vivo*. Our previous study showed that the $1/T_2$ relaxation rate is substantially affected by stability of PEG-coated SPIONs.[12] Our SPIONs are stable in pH 9 for years (data no shown). The zeta-potential values of SPIONs in pH 9 solution are −26, −18, and −8 mV for 2-MEA, PEG 2K, and PEG 10K SPIONs, respectively. The particle size increases over hours in DMEM because of the high salt concentration. The high salt concentration shields electrostatic interaction between particles, which leads to aggregation. Interestingly, when serum is added to DMEM (DMEM+BCS), which results in a more physiologically relevant condition, particle size remains at approximately 200 nm for 12h for all three kinds of SPIONs. The zeta-potential value of SPIONs in DMEM+BCS is −38 mV, which is more negative than values of SPIONs in pH 9 solution. More negative zeta-potentials in the presence of serum indicate that negatively charged biomolecules such as albumin are adsorbed onto the nanoparticles, resulting in electrostatic stabilization of the nanoparticles. The adsorption of biomolecules can be verified by TGA analysis results (Table 2). Weight percentage loss of the surface coating for 2-MEA SPIONs in DMEM+BCS, for example, increased from 13.1% in pH 9 solution to 57.2%. Compared to DMEM (23.1%), the difference is substantial, indicating that biomolecules, in addition to glucose in DMEM, adsorbed onto the particle surface in DMEM+BCS. Surface saturation with BCS-containing medium can also be favorable for reducing nonspecific cellular uptake and cytotoxicity because it presumably masks the reactive surface of nanoparticles, thus preventing the interaction between cell and nanoparticle.[14] However, further stability studies for targeted SPIONs will be necessary because plasma protein adsorption may interfere with targeting ligands on the particle surface to bind to targeted receptors.

The normal dose of SPIONs administered intravenously is 0.1−0.5 mg/kg,[22] but higher dosages may be required to maximally benefit a therapeutic or diagnostic application, especially for targeted SPIONs. Therefore, the study of SPION cytotoxicity *in vitro* is necessary to determine a cytotoxic dose limit of the SPIONs prior to *in vivo* studies. It has been shown that cytotoxicity of uncoated SPIONs occurs at concentrations higher than 50 ppm Fe.[23]

Our preliminary results of cytotoxicity with citric acid-coated SPIONs at a concentration of 1000 ppm Fe to VSMCs also show that our nanoparticles have a detrimental effect on VSMCs, causing cytoplasmic vesicles to form and coalesce, eventually leading to cell death. VSMCs incubated with citric acid-coated SPIONs began producing vacuoles as early as 5 h after particle exposure and over time these vacuoles grow and coalesce, eventually resulting in cell death. Unlike citric acid-coated SPIONs, PEGylated SPIONs did not show large vacuole formation during the first 5 h. However, we observed small vesicle formation at 5 h incubation, mostly at the 500 ppm Fe concentrations and to a lesser extent at 100 ppm Fe (Figure 5). According to the Live/Dead assay results (Figure 2), toxicity of PEGylated SPIONs was influenced by the SPION concentration to which the cells were exposed. Cytotoxicity with 100 ppm Fe of SPIONs was less than that of 500 ppm Fe of SPIONs. Time-lapse movies also showed that inhibition of cell proliferation was observed over 24 h at 500 ppm Fe. Cells were unable to attach to a well surface, which could explain the cell death observed at 500 ppm Fe. When nanoparticle clearance was simulated by washing, more cells survived after 24 h, both at 100 and 500 ppm Fe of PEGylated SPIONs. Upon nanoparticle clearance, cells were able to attach to a surface again, cell morphology improved, and cell death was substantially reduced. The whole cell area and whole cell perimeter data also support effects of SPION concentrations and clearance on enhancing cell viability, probably because high concentration of SPIONs themselves could be detrimental to cells, or high concentrations SPIONs on cell culture dish surfaces prevent cells from attaching.[24] As DLS stability data support the fast aggregation of SPIONs observed at high concentrations, this aggregation may have also influenced the cell viability.

Concentration of SPIONs at 100 ppm Fe showed better results than 500 ppm Fe in terms of cell viability and was also sufficient for enhanced contrast MRI imaging. The T_2 contrast images with 500 ppm Fe in Figure 1 were already saturated, meaning that the $1/T_2$ relaxation rate was no longer linearly proportional to concentration. The $1/T_2$ relaxivity of the various PEG MW SPIONs ranged from 0.6456 to 1.049 $s^{-1}ppm^{-1}$. For 100 ppm Fe, the $1/T_2$ relaxation rate ranged from 64.56 to 104.9 s^{-1}, which is much higher than the surrounding body tissue; thus, it can provide sufficient contrast. The relaxivity values are comparable to or higher than commercially used contrast agents Feridex and Resovist, which are 0.42 $s^{-1}ppm^{-1}$ (98.3 $s^{-1}mM^{-1}$) and 0.65 $s^{-1}ppm^{-1}$ (150 $s^{-1}mM^{-1}$), respectively. The $1/T_2$ relaxivity values of the various PEG MWs SPIONs generally decreased as the PEG coating MW increased, a result in agreement with LaConte et al.[9] According to their simulation results, this decrease in relaxivity values is attributed to combined effects of water exclusion and slow diffusion due to the coating. The relaxivity can also be affected by the iron core size. Future studies of SPIONs optimization with different core sizes are thus necessary.

Lastly, nonspecific cellular uptake should be taken into account when optimizing contrast agents because nonspecific internalization makes it difficult to diagnose and treat specific desired target areas and is therefore undesirable. Nonspecific cellular uptake occurs easily via particle adsorption to cell surface. This adsorption can be reduced by steric hindrance provided by PEG coatings.[25] With 100 ppm Fe of various PEG MWs SPIONs, we did not observe any particles internalized in cells within 1 h. However, after 5 h, particles covered most parts of the cell, with the exception of PEG 2K SPIONs. Cell viability of PEG 2K SPIONs was also highest among those particles tested. With 500 ppm Fe, the majority of particles appeared to be localized in the perinuclear region of the cell. Particles covered the nuclear region, especially for PEG 10K SPIONs. A recent study demonstrated a relationship between cytotoxicity and nuclear permeabilization.[26] Although it is not certain which factor affects the other parameters, we found that cell viability with PEG 10K at 500 ppm Fe after 5 h incubation was the lowest (Figure 2), which is consistent with the study from Grandinetti et al.[26] In the future, comparisons of targeted SPIONs to examine cytotoxicity and specific internalization via upregulated receptors on VSMCs are necessary to optimize targeted contrast agents.

Overall, our study showed the effect of the particle coating and the concentration on nanoparticle performance and interaction with cells. In general, 100 ppm Fe of the PEG 2K showed good stability and magnetic contrast with the least cytotoxicity and nonspecific cellular uptake in VSMCs. The results may be valid for this specific cell type and may vary with different cell types. Because the composition of cellular membrane where nanomaterial surface contacts is different for each cell type, the effect of the particle coating and the dose on cell viability or cellular uptake can also depend on the cell type.[27,28]

5. Conclusions

Monodisperse SPIONs were coated with various molecular weights of PEG, and the PEGylated SPIONs were characterized and examined with VSMCs for potential use as atherosclerosis MRI contrast agents. Different concentrations (100 and 500 ppm Fe) of SPIONs were tested for stability, T_2 contrast, cytotoxicity, and cellular uptake to determine optimal conditions for the application. To the best of our knowledge, this is the first report to systematically study the effect of PEG coating on SPIONs and the concentration of SPIONs on overall nanoparticle performance. In general, 100 ppm Fe of the PEG 2K showed good stability and magnetic contrast with the least cytotoxicity and nonspecific cellular uptake in VSMCs. Clearance of particles by circulation was also simulated, showing substantially higher cell viability than without clearance for all formulations. Our investigation provides insight into the potential safety and application of nanoparticles in the clinic.

Acknowledgments

This research was supported in part by a College of Engineering Distinguished Faculty Fellowship to J.Y.W. and by NIH HL 072900 and by NSF 0910908. Tuan Pham was supported in part by NIH/NIGMS T32 GM008764, NIH/NIAID T32 AI089673, and NIH 5P50HL083801. Jared B. Smith was supported by NIH/NHLBI HL072900-S. Christopher A. Sucato was supported by NIH/NHLBI T32 HL007224.

References

1. Lloyd-Jones D, Adams R, Carnethon M, De Simone G, Ferguson TB, Flegal K, et al. Heart disease and stroke statistics--2009 update: a report from the American Heart Association Statistics Committee and Stroke Statistics Subcommittee. Circulation. 2009; 119:480–486. [PubMed: 19171871]
2. van der, Wal AC.; Becker, AE.; van der, Loos CM.; Das, PK. Site of intimal rupture or erosion of thrombosed coronary atherosclerotic plaques is characterized by an inflammatory process irrespective of the dominant plaque morphology. Circulation. 1994; 89:36–44. [PubMed: 8281670]
3. Farb A, Burke AP, Tang AL, Liang TY, Mannan P, Smialek J, et al. Coronary plaque erosion without rupture into a lipid core. A frequent cause of coronary thrombosis in sudden coronary death. Circulation. 1996; 93:1354–1363. [PubMed: 8641024]
4. Saam, T.; Kerwin, WS.; Yuan, C. Vascular Imaging. In: GL, Bowlin; GE, Wnek, editors. Encyclopedia of biomaterials and biomedical engineering. New York: Marcel Dekker; 2004.
5. Shan L. Molecular Imaging and Contrast Agent Database (MICAD). :2004–2013.
6. Bjornerud A, Johansson L. The utility of superparamagnetic contrast agents in MRI: theoretical consideration and applications in the cardiovascular system. NMR in biomedicine. 2004; 17:465–477. [PubMed: 15526351]
7. Wang YX. Superparamagnetic iron oxide based MRI contrast agents: Current status of clinical application. Quantitative imaging in medicine and surgery. 2011; 1:35–40. [PubMed: 23256052]
8. Allkemper T, Bremer C, Matuszewski L, Ebert W, Reimer P. Contrast-enhanced blood-pool MR angiography with optimized iron oxides: effect of size and dose on vascular contrast enhancement in rabbits. Radiology. 2002; 223:432–438. [PubMed: 11997549]
9. LaConte LEW, Nitin N, Zurkiya O, Caruntu D, O'Connor CJ, Hu XP, et al. Coating thickness of magnetic iron oxide nanoparticles affects R-2 relaxivity. Journal of Magnetic Resonance Imaging. 2007; 26:1634–1641. [PubMed: 17968941]
10. Tong S, Hou S, Zheng Z, Zhou J, Bao G. Coating optimization of superparamagnetic iron oxide nanoparticles for high T2 relaxivity. Nano letters. 2010; 10:4607–4613. [PubMed: 20939602]
11. Petri-Fink A, Steitz B, Finka A, Salaklang J, Hofmann H. Effect of cell media on polymer coated superparamagnetic iron oxide nanoparticles (SPIONs): colloidal stability, cytotoxicity, and cellular uptake studies. European journal of pharmaceutics and biopharmaceutics : official journal of Arbeitsgemeinschaft fur Pharmazeutische Verfahrenstechnik eV. 2008; 68:129–137.
12. Park Y, Whitaker RD, Nap RJ, Paulsen JL, Mathiyazhagan V, Doerrer LH, et al. Stability of Superparamagnetic Iron Oxide Nanoparticles at Different pH Values: Experimental and Theoretical Analysis. Langmuir. 2012; 28:6246–6255. [PubMed: 22409538]
13. Laurent S, Forge D, Port M, Roch A, Robic C, Vander Elst L, et al. Magnetic iron oxide nanoparticles: synthesis, stabilization, vectorization, physicochemical characterizations, and biological applications. Chemical reviews. 2008; 108:2064–2110. [PubMed: 18543879]
14. Singh N, Jenkins GJ, Asadi R, Doak SH. Potential toxicity of superparamagnetic iron oxide nanoparticles (SPION). Nano reviews. 2010:1.
15. Lattuada M, Hatton TA. Functionalization of monodisperse magnetic nanoparticles. Langmuir. 2007; 23:2158–2168. [PubMed: 17279708]
16. Chithrani BD, Ghazani AA, Chan WCW. Determining the size and shape dependence of gold nanoparticle uptake into mammalian cells. Nano Letters. 2006; 6:662–668. [PubMed: 16608261]
17. Wilhelm C, Billotey C, Roger J, Pons JN, Bacri JC, Gazeau F. Intracellular uptake of anionic superparamagnetic nanoparticles as a function of their surface coating. Biomaterials. 2003; 24:1001–1011. [PubMed: 12504522]
18. Dumazet-Bonnamour I, Le Perchec P. Colloidal dispersion of magnetite nanoparticles via in situ preparation with sodium polyoxyalkylene di-phosphonates. Colloids and Surfaces a-Physicochemical and Engineering Aspects. 2000; 173:61–71.
19. Rootman DS, Hasany SM, Basu PK. A morphometric study of endothelial cells of human corneas stored in MK media and warmed at 37 degrees C. The British journal of ophthalmology. 1988; 72:545–549. [PubMed: 3415947]

20. Garcia-Herreros M, Leal CL. Sperm morphometry: a tool for detecting biophysical changes associated with viability in cryopreserved bovine spermatozoa. Andrologia. 2013
21. Wahajuddin , Arora S. Superparamagnetic iron oxide nanoparticles: magnetic nanoplatforms as drug carriers. International journal of nanomedicine. 2012; 7:3445–3471. [PubMed: 22848170]
22. Elias A, Tsourkas A. Imaging circulating cells and lymphoid tissues with iron oxide nanoparticles. Hematology / the Education Program of the American Society of Hematology American Society of Hematology Education Program. 2009:720–726. [PubMed: 20008258]
23. Berry CC, Wells S, Charles S, Curtis AS. Dextran and albumin derivatised iron oxide nanoparticles: influence on fibroblasts in vitro. Biomaterials. 2003; 24:4551–4557. [PubMed: 12950997]
24. Frank JA, Miller BR, Arbab AS, Zywicke HA, Jordan EK, Lewis BK, et al. Clinically applicable labeling of mammalian and stem cells by combining superparamagnetic iron oxides and transfection agents. Radiology. 2003; 228:480–487. [PubMed: 12819345]
25. Kelf TA, Sreenivasan VK, Sun J, Kim EJ, Goldys EM, Zvyagin AV. Non-specific cellular uptake of surface-functionalized quantum dots. Nanotechnology. 2010; 21:285105. [PubMed: 20585157]
26. Grandinetti G, Smith AE, Reineke TM. Membrane and nuclear permeabilization by polymeric pDNA vehicles: efficient method for gene delivery or mechanism of cytotoxicity? Molecular pharmaceutics. 2012; 9:523–538. [PubMed: 22175236]
27. Rauch J, Kolch W, Mahmoudi M. Cell Type-Specific Activation of AKT and ERK Signaling Pathways by Small Negatively-Charged Magnetic Nanoparticles. Scientific Reports. 2012; 2:868. [PubMed: 23162692]
28. Laurent S, Burtea C, Thirifays C, Ha¨ feli UO, Mahmoudi M. Crucial Ignored Parameters on Nanotoxicology: The Importance of Toxicity Assay Modifications and “cell vision”. PLoS ONE. 2012; 7:e29997. [PubMed: 22253854]

- SPIONs with various PEG MWs coating for potential atherosclerosis MRI contrast agents.
- Optimal condition determined for stability, T2 contrast, cytotoxicity, and cellular uptake.
- 100 ppm Fe SPION with PEG 2K showed the optimal condition for the application.
- Cell viability increased when SPIONs were washed (simulating circulation).

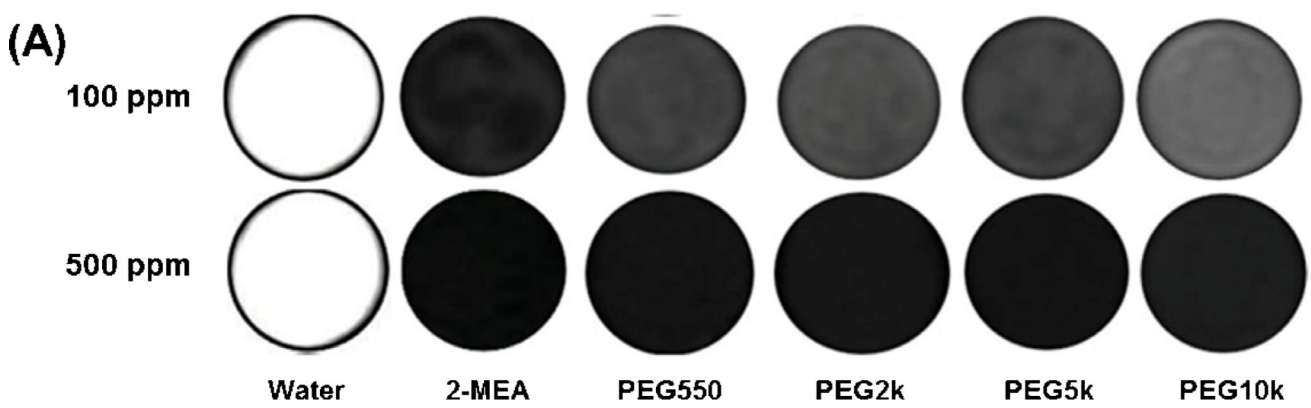

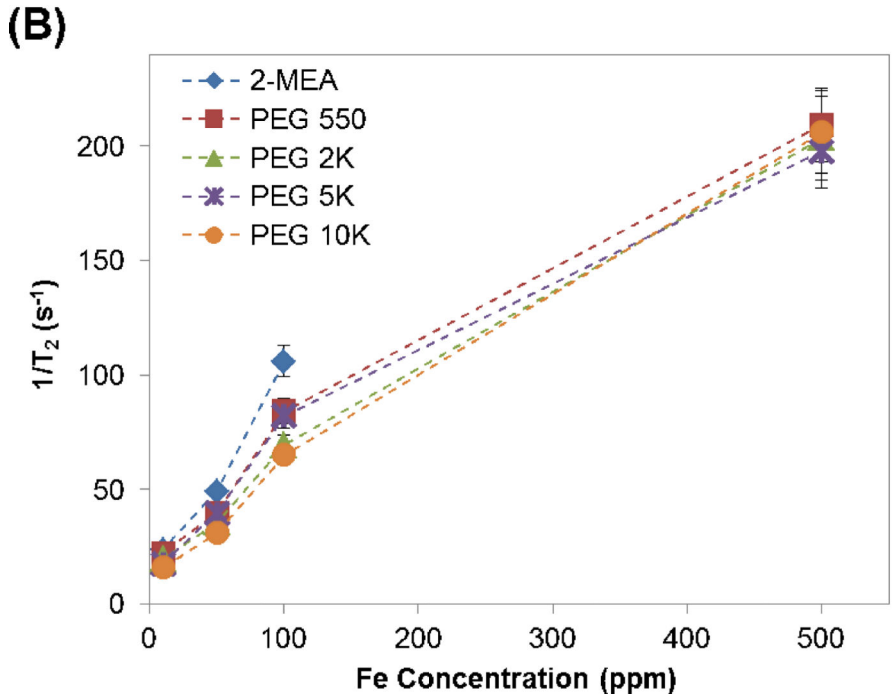

(C)

SPION Coating	R_2 relaxivity ($s^{-1}ppm^{-1}$)
2-MEA	1.049
PEG 550	0.8379
PEG 2K	0.7021
PEG 5K	0.8176
PEG 10K	0.6456

Figure 1.

(A) MRI slice of deionized water and SPIONs coated with various PEG MWs in deionized water at 100 ppm Fe and 500 ppm Fe. Black lines added as a visual aid. (B) $1/T_2$ relaxation rate of SPIONs as a function of iron concentration. (C) R_2 relaxivity in $s^{-1}ppm^{-1}$ for various PEG MW of SPION coating.

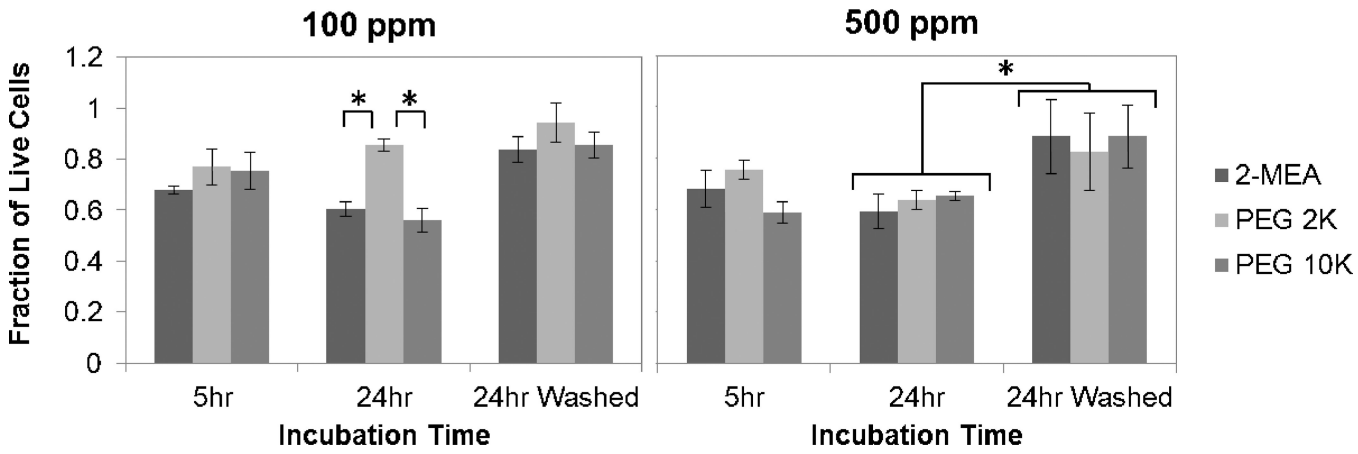

Figure 2.

Live/Dead Assay of VSMCs. Cells were incubated with SPIONs in DMEM for 2-MEA, PEG 2K, PEG 10K at 100 ppm Fe and 500 ppm Fe. “24 h wash” indicates cells exposed to SPIONs for 1 h, and then washed and replaced with fresh media for the next 23 h.*Significant difference for $p < 0.05$.

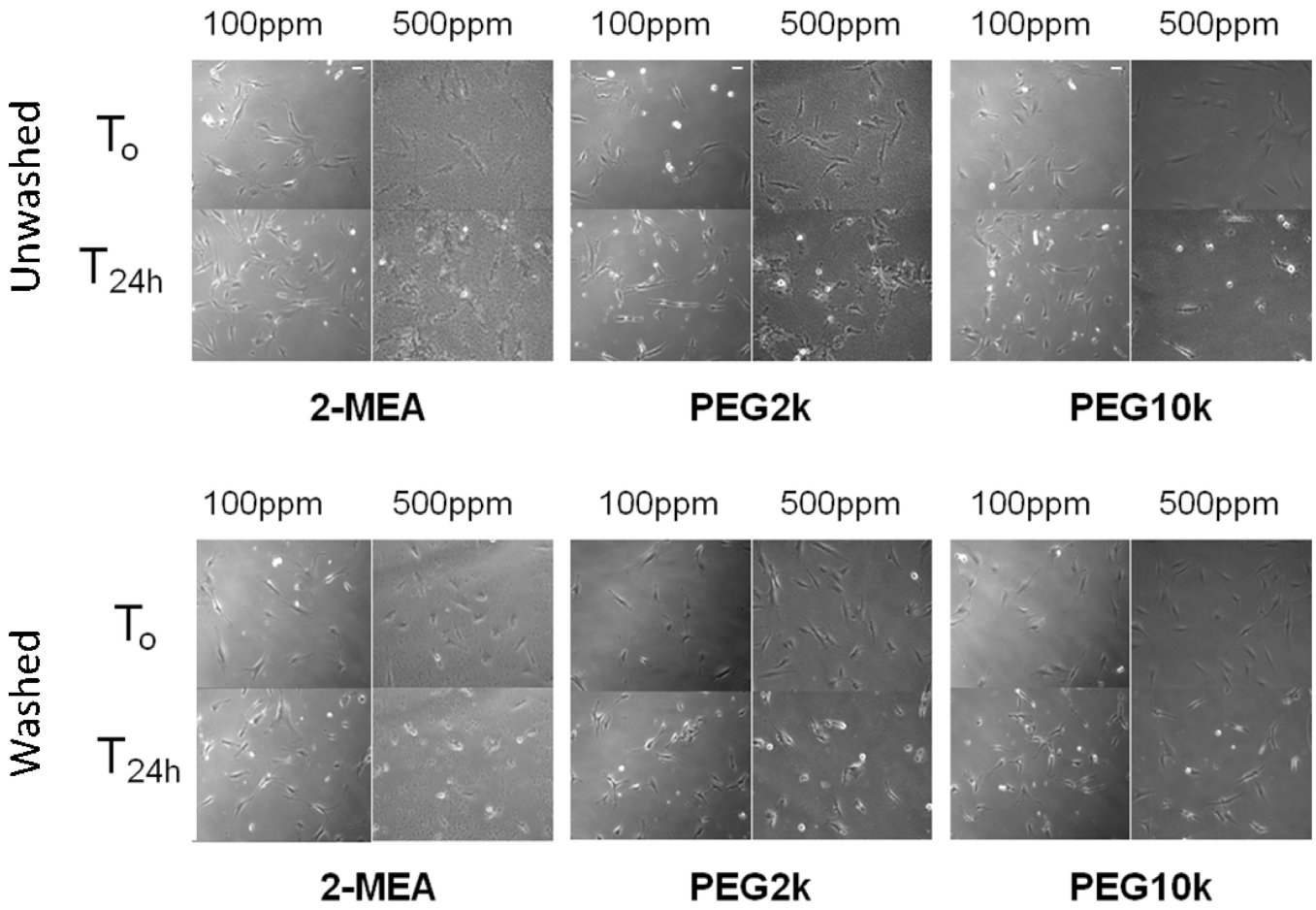

Figure 3.

Time-lapse representative images of VSMCs with 2-MEA, PEG 2K, and PEG 10K SPIONs incubation at 0 h (T_0), 24 h (T_{24h}). Cells were exposed to SPIONs either for 24 h (top: Unwashed) or 1 h and washed with media (bottom: Washed). This study was performed in DMEM at 100 ppm Fe and 500 ppm Fe of SPION concentrations.

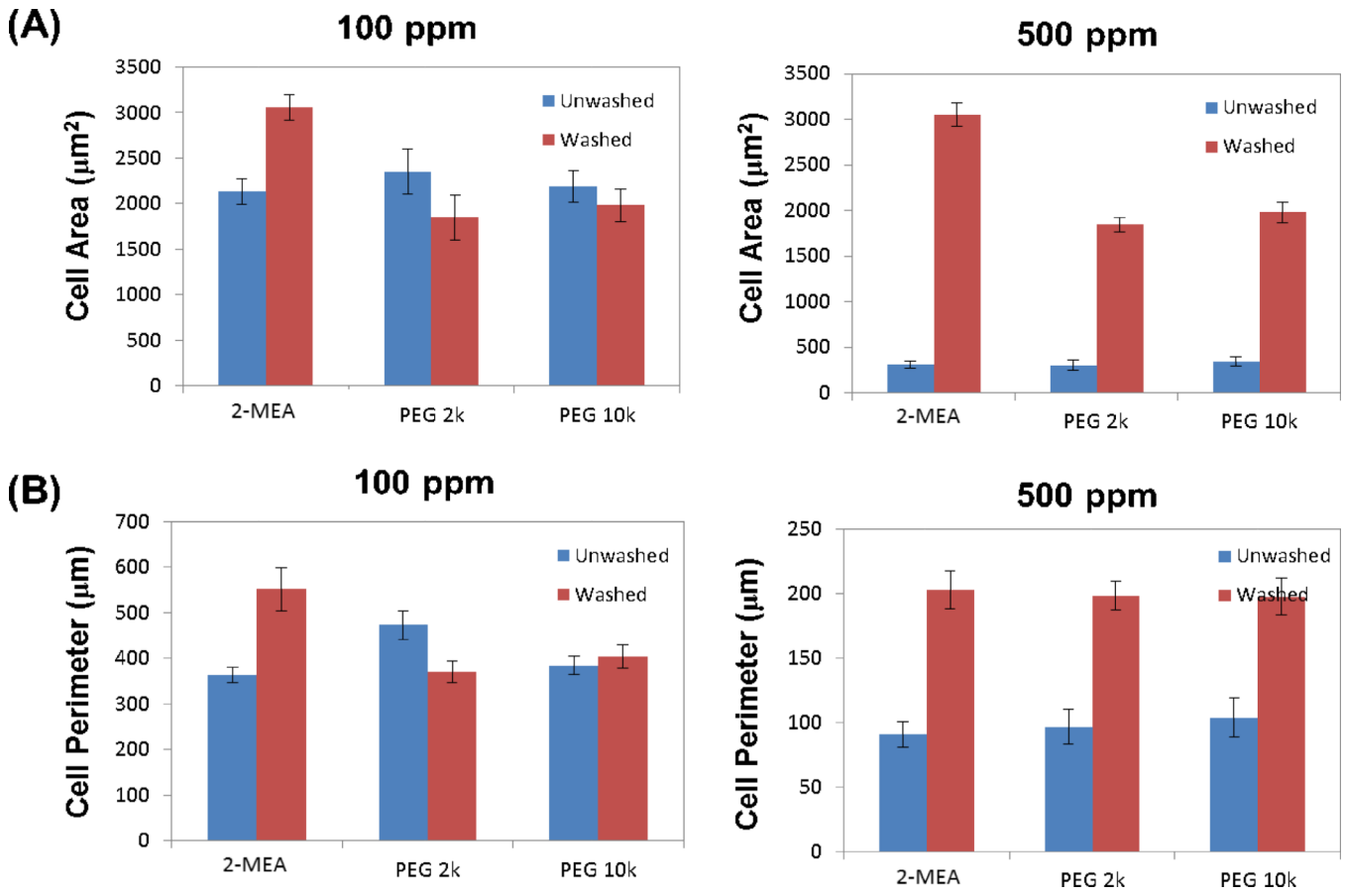

Figure 4.

Quantification of morphological characteristics of VSMCs from time-lapse images (Figure 3) at 24 h (T_{24h}): (A) whole cell area; (B) whole cell perimeter. The conditions are the same as in Figure 3.

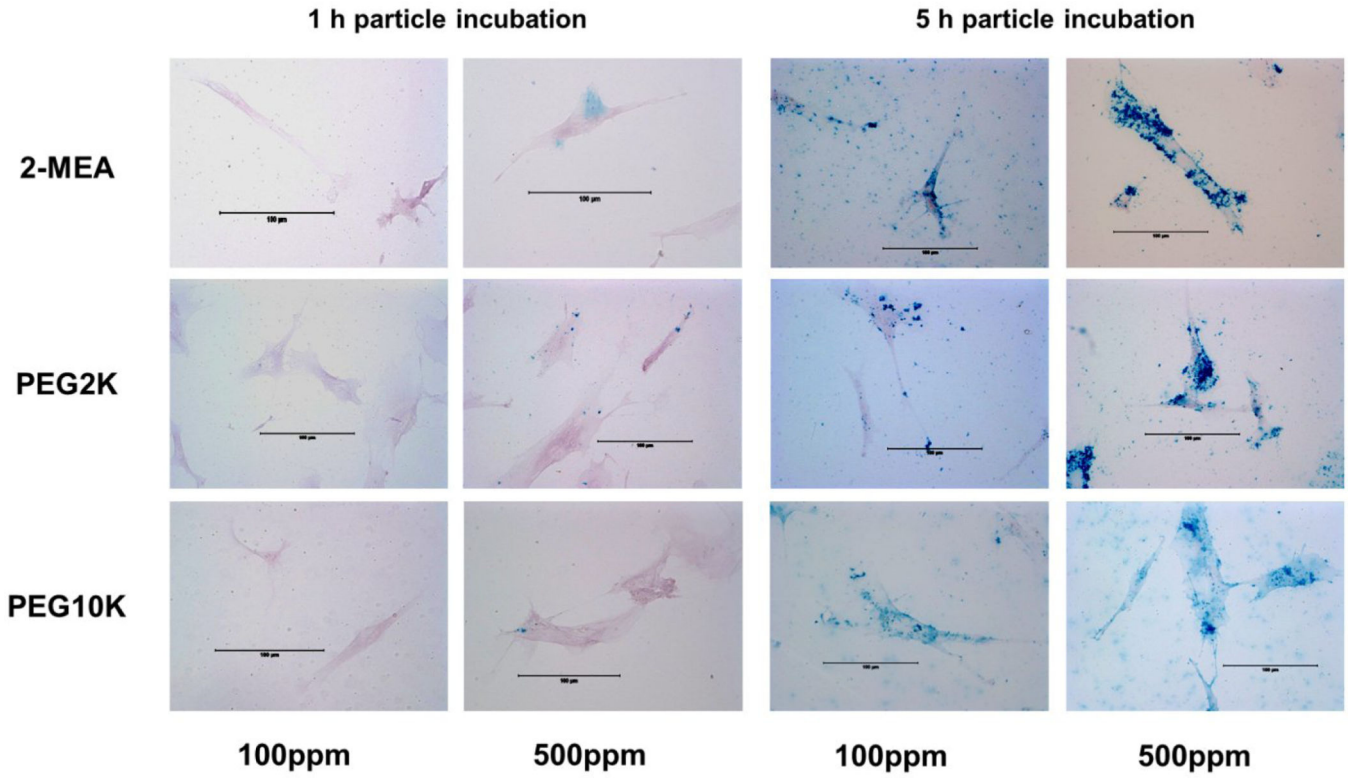

Figure 5.
Prussian blue assay of VSMCs. Cells were incubated with 2-MEA, PEG 2K, or PEG 10 K SPIONs in DMEM at 100 ppm Fe and 500 ppm Fe for 1 h and 5 h.

Table 1

. Elemental analysis results of SPIONs and calculation of number of surface molecules.

Nanoparticle coating	% carbon	Molecules per nanoparticle	Surface density (molecules/nm^2)	Distance between grafting sites (nm)
Citric acid	4.6	968	3.52	0.410
2-MEA	5.7	925	3.37	0.420
PEG 550	6.3	282	1.03	1.39
PEG 2K	6.6	87.5	0.319	4.50
PEG 5K	6.6	35.2	0.128	11.2
PEG 10K	7.7	21.3	0.0774	18.5

Table 2

Thermogravimetric analysis (TGA) results of SPIONs and calculation of number of surface molecules. Percentages of weight loss of 2-MEA, PEG 2K, and PEG 10K SPIONs stored in DMEM with and without BCS were also measured.

Nanoparticle coating	Molecules per nanoparticle	Surface density (molecules/nm2)	% Weight loss		
			pH 9	DMEM	DMEM+BCS
Citric Acid	1430	5.22	18.7	N/A	N/A
2-MEA	839	3.06	13.1	23.1	57.2
PEG 550	270	0.982	13.2	N/A	N/A
PEG 2K	156	0.567	20.6	29.8	53.0
PEG 5K	323	1.18	56.1	N/A	N/A
PEG 10K	170	0.620	56.9	24.4	56.2

Table 3

Average hydrodynamic diameters (D_H in nm) of 2-MEA, PEG 2K and PEG 10K SPIONs over 12 h in pH 9 buffer solution, DMEM, and DMEM + BCS, at two different concentrations (100 and 500 ppm Fe), measured by DLS.

			0 h	2 h	4 h	8 h	12 h
2-MEA	pH 9	100 ppm	135	132	126	132	125
		500 ppm	127	127	121	124	125
	DMEM	100 ppm	442	728	738	720	722
		500 ppm	815	957	974	988	909
	DMEM + BCS	100 ppm	229	232	220	235	232
		500 ppm	242	255	254	258	269
PEG 2K	pH 9	100 ppm	145	161	165	159	142
		500 ppm	142	141	146	145	152
	DMEM	100 ppm	562	730	721	796	830
		500 ppm	919	1034	973	1098	1058
	DMEM + BCS	100 ppm	226	238	224	226	227
		500 ppm	245	259	253	251	263
PEG 10K	pH 9	100 ppm	109	114	120	118	113
		500 ppm	125	129	122	125	127
	DMEM	100 ppm	690	820	851	825	798
		500 ppm	823	837	869	1137	1027
	DMEM + BCS	100 ppm	218	219	217	214	212
		500 ppm	233	247	235	244	257

Colloids Surf B Biointerfaces. Author manuscript; available in PMC 2015 July 01.